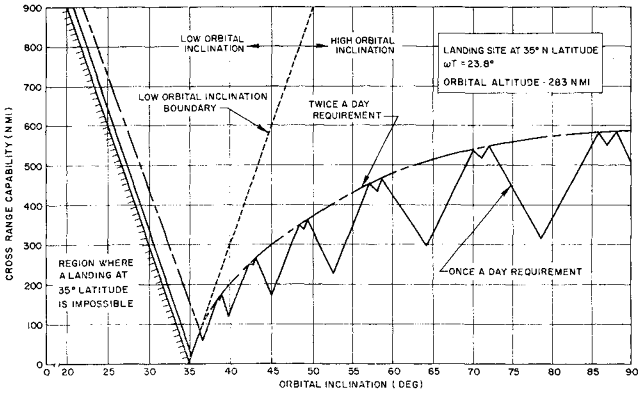

Fig. 3 Cross-range coverage to insure one and two landing opportunities each day.

An application of the latitude coverage thus determined is shown in Fig. 3. The curves given in Fig. 3 represent the cross range required to assure at least one and two landing opportunities each day, respectively, for a landing site located at a latitude of 35° (Edwards Air Force Base) as a function of orbital inclination. Generation of such curves requires the determination of the orbit trace spacing, at the landing site latitude, produced within the time period in which the landing opportunities are to be assured. Detailed procedures for this step are outlined in Ref. 3.

References

[1] Baradell, D. L. and McLellan, C. H., "Lateral-range and hypersonic lift-drag-ratio requirements for efficient ferry service from a near-earth manned space station," *AIAA Second Manned Space Flight Symposium* (American Institute of Aeronautics and Astronautics, New York, 1963).

[2] Boyle, E. J., Jr., "Recall and return of a manned vehicle from orbit," *Advances in the Astronautical Sciences: Space Rendezvous Rescue and Recovery* (American Astronautical Society, New York, 1963) Vol. 16, Part 1, p. 829.

[3] Stern, R. G. and Chu, S. T., "Landing site coverage for orbital lifting re-entry vehicles," Aerospace Corp., Rept. TDR-169(3530-10) TN-1 (April 1963).

Lunar Landing Guidance Using Cross-Product Steering

William J. Budurka*
and Norman L. Pleszkoch†
International Business Machines Corporation, Owego, N. Y.

A TERMINAL guidance technique is presented which insures a soft-landing at a preselected site on the lunar surface. The technique employs two feedback guidance channels to achieve continuous thrust vector control throughout the powered portion of the descent. One channel nullifies an error generated by application of a form of cross-product steering, thereby insuring passage of the vehicle trajectory through the desired landing site with a small horizontal velocity component (less than 2 fps) to avoid tipping. The other channel nullifies a second error signal, insuring a terminal value of vertical velocity which is within the bound (15 fps) required for a soft-landing. The simulation results presented are necessarily preliminary but provide a quantitative demonstration of feasibility.

Received January 31, 1964; revision received April 6, 1964.
* Staff Engineer, Space Guidance Center.
† Technical Associate, Space Guidance Center.

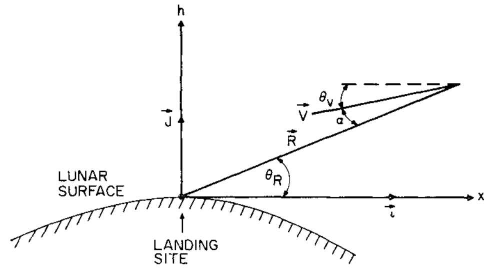

Fig. 1 Landing geometry.

Cross-Product Steering: Basic Relations

In order to arrive at a set of guidance equations having the simplest po sible form, it is assumed that landing occurs in a Cartesian coordinate system, with origin of the x-h plane at the desired landing site—an assumption that is justified for small angular travel during powered descent and that becomes more accurate as the landing site is approached.

The concept of cross-product steering for the planar case is illustrated by Fig. 1, which shows that the spacecraft will be forced to pass through the landing site if its velocity vector is aligned to the range vector, i.e., if $\tan\theta_R = \tan\theta_v$, which can be insured by nullifying the error

$$\epsilon_p = h\dot{x} - x\dot{h} \tag{1}$$

Forcing ϵ_p to zero is equivalent to forcing the vector cross product of **V** and **R** to zero

$$\mathbf{V} \times \mathbf{R} = VR\sin\alpha\cdot\mathbf{k} = \langle\dot{x}\mathbf{i} + \dot{h}\mathbf{j}\rangle \times \langle x\mathbf{i} + h\mathbf{j}\rangle = \langle h\dot{x} - x\dot{h}\rangle\cdot\mathbf{k} \tag{2}$$

Notice that if ϵ_p is maintained at zero, the nominal vehicle trajectory is a straight line. Equation (2) can be modified to give alternate preferred trajectories that allow the landing site to be approached along a more vertical path; this approach is more desirable if the vehicle is expected to hover before landing. The modification is achieved by setting

$$\beta\tan\theta_R = \tan\theta_v \qquad \beta = \text{const} \tag{3}$$

so that

$$\epsilon_p = \beta h\dot{x} - x\dot{h} \tag{4}$$

If this $\epsilon_p = 0$ throughout the descent, the trajectory is given by

$$h = (h_0/x_0^{\beta})x^{\beta} = Kx^{\beta} \tag{5}$$

where h_0 and x_0 are the initial altitude and position. For fixed initia' position, and $0 < \beta \leq 1$, a family of trajectories is obtained (Fig. 2a). Alternately, if β is fixed but initial conditions are varied, a different family is generated (Fig. 2b). For each case, whenever $0 < \beta < 1$, the trajectories have the property that $\dot{x} \to 0$ as $x \to 0$.

Nullification of ϵ_p insures passage of the spacecraft trajectory through the desired landing site but does not simultaneously insure that a soft landing will be achieved. That

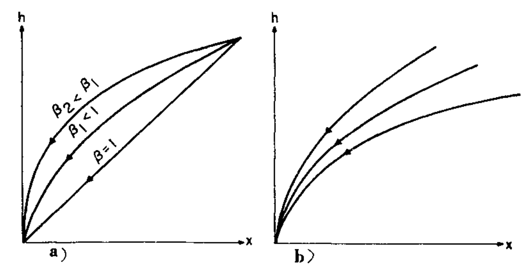

Fig. 2 Nominal ideal trajectories for $\epsilon_p = 0$: *a*) for fixed h_0x_0, variable β; *b*) for fixed β, variable h_0x_0.

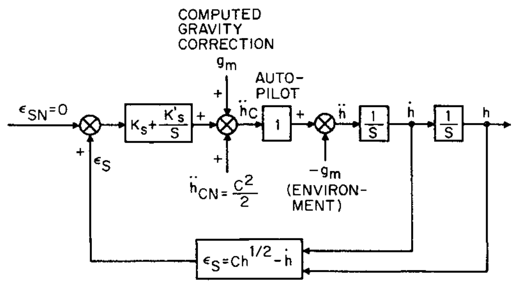

Fig. 3 Soft-landing control, vertical channel: assuming ideal autopilot.

is, another error signal, say, ϵ_s, must be defined such that if $\epsilon_s = 0$ the vertical velocity component must lie within soft-landing limits. Several expressions for ϵ_s are suitable, the choice being determined by simplicity of form, fuel consumption, flight time, etc. In this paper, ϵ_s is defined:

$$\epsilon_s = Ch^{1/2} - \dot{h} \qquad C = \text{const} \tag{6}$$

which is equivalent to commanding a constant vertical acceleration component of magnitude $C^2/2$.

The approach taken in this paper, simultaneously to maintain the error signals ϵ_p and ϵ_s at zero, is to compute nominal values for commanded horizontal $\ddot{x}_c$ and vertical $\ddot{h}_c$ components of acceleration and add correction terms whose values depend upon the magnitudes of the computed errors ϵ_p and ϵ_s, respectively. The signs of the correction terms are chosen so that the errors are gradually reduced to zero on a closed-loop basis.

Vertical and Horizontal Channels

A simplified diagram of the vertical (soft-landing) channel, assuming an ideal (unity transfer function) autopilot (Fig. 3), is obtained by the following reasoning: If $\epsilon_s \equiv 0$ throughout the flight, then the required vertical acceleration component is just equal in magnitude to $\frac{1}{2}C^2 + g_m$, where g_m is the gravity of moon. However, if the chosen initial conditions, or some disturbance, causes $\epsilon_s \neq 0$, then ϵ_s can be forced to zero by commanding a vertical acceleration component equal to the nominal value just given, plus an amount proportional to a weighted linear combination of ϵ_s, plus the integral of ϵ_s:

$$\ddot{h}_C = \tfrac{1}{2}C^2 + g_m + K_s\epsilon_s + K_s'\textstyle\int \epsilon_s dt \tag{7}$$

In the "steady-state" when $\epsilon_s = 0$, the third term of Eq. (7) is dropped.

Obviously, the chosen values for the weighting constants K_s, K_s' determine the time history of the error ϵ_s as it is being forced to zero. For example, if $K_s = 0$ and ϵ_s is initially large, an instantaneous correction to the nominal acceleration command cannot occur because of the finite time required for the integrator to build up a value. A faster response can be achieved by increasing K_s', but this approach is inadequate because of oscillations in the error response. However, by introducing $K_s \neq 0$, the response time can be reduced without producing oscillations, i.e., the term proportional to ϵ_s in the expressions for $\ddot{h}_c$ provides for a damping effect.

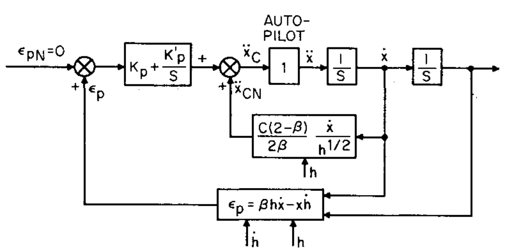

Fig. 4 Landing site location control, horizontal control: assuming ideal autopilot.

A simplified diagram of the horizontal channel, assuming an ideal (unit transfer function) autopilot, is shown in Fig. 4. The cross-product error ϵ_p is used to compute a correction to the nominal value of horizontal acceleration analogous to use of ϵ_s in Fig. 3. The nominal value of horizontal acceleration may be determined by assuming that in the ideal situation $\epsilon_p \equiv 0$, which implies that $\dot{\epsilon}_p$ is also zero. Thus, if the expression for ϵ_p is differentiated and set equal to zero, the following expression for the horizontal acceleration component (the *nominal* value required) is obtained:

$$\ddot{x}_{Cn} = [x\ddot{h} + (1 - \beta)\dot{x}\dot{h}]/\beta h \tag{8}$$

This expression can be simplified if $\dot{h}$ and $\ddot{h}$ are replaced by those values that would result if the error ϵ_s is identically zero, i.e., $Ch^{1/2}$ and $C^2/2$, respectively; then, by assuming $\epsilon_p = 0$, a simplified expression for $\ddot{x}_{Cn}$ is obtained:

$$\ddot{x}_{Cn} = [C(2 - \beta)\dot{x}]/2\beta h^{1/2} \tag{9}$$

As shown in Fig. 4, the total horizontal acceleration component commanded (assuming negligible gravity in the x direction) is

$$\ddot{x}_C = [C(2 - \beta)\dot{x}]/2\beta h^{1/2} + K_p\epsilon_p + K_p'\textstyle\int \epsilon_p dt \tag{10}$$

The weighting constants K_p, K_p' affect the horizontal channel in the same way that K_s and K_s' affect the vertical one.

Simulation Results

The guidance technique described here has been studied utilizing a three-degree-of-freedom (i.e., motion in a vertical plane over a "flat" moon) analog-simulation program, in which the spacecraft was controlled by a gimballed (±10°) throttleable (5000- to 50,000-lb-thrust) rocket engine. The acceleration commands given by Eqs. (7) and (10) were employed somewhat differently than in Figs. 3 and 4. The desired thrust angle is obtained by making the engine gimbal deflection proportional to the difference between the ideal (γ_C = arc tan $\ddot{h}_C/\ddot{x}_C$) and actual (γ) values of spacecraft attitude plus attitude rate. The desired thrust magnitude is obtained by throttling the engine to give total acceleration equal to $(\ddot{x}_C^2 + \ddot{h}_C^2)^{1/2}$.

Simulation results show that the technique performs well for a value range of initial position (x_0 = 90–100 miles; h_0 = 80,000–100,000 ft) using one set of empirically determined

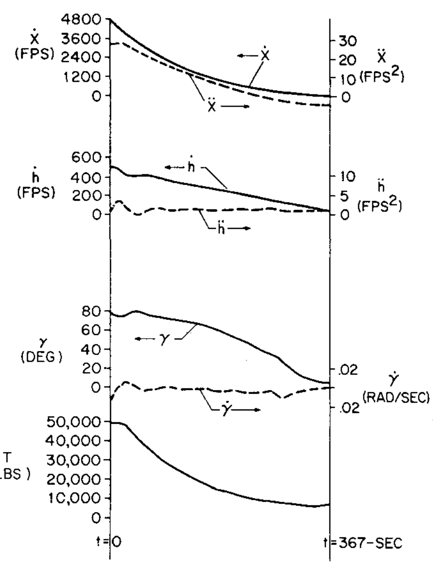

Fig. 5 Typical time histories: initial altitude 100,000 ft, initial position 100 miles.

values (from a series of computer runs) for the weighting constants: $K_p = 5 \times 10^{-4}$, $K_p' = 5 \times 10^{-6}$, $K_s = 10^{-1}$, and $K_s' = 5 \times 10^{-3}$ with C and β set arbitrarily at 1.50 and 0.50, respectively. For example, in a typical run (for which the initial conditions are $\dot{h}_0 = 500$ fps; $h_0 = 100{,}000$ ft; $\dot{x}_0 = 5000$ fps; $x_0 = 100$ miles, $I_{sp} = 423.5$; and, initial mass = 1500 slugs) the conditions upon reaching an altitude of 2000 ft are: $x = 120$ ft; $\dot{x} = 30$ fps; $\dot{h} = 67$ fps; altitude = 7° from vertical; ΔV = characteristic velocity = 5800 fps; and elapsed time = 367 sec. The time histories of certain variables along this trajectory are shown in Fig. 5. The simulation run presented here was terminated early because of the tendency of $\ddot{x}_C$ computed from Eq. (10) to take on large erroneous values as h approached zero. This difficulty is easily resolved by holding the denominator of Eq. (10) fixed whenever h decreases below a threshold value.

A Method of Calculating Rocket Plume Radiation to the Base Region

C. L. Tien* and M. M. Abu-Romia†
University of California, Berkeley, Calif.

In the design of large booster vehicles, it is recognized that the base regions should be protected against heating by the rocket exhaust plumes. The present work describes an analytical attempt to calculate the radiative energy transfer from rocket exhaust plumes to the base regions by use of idealized physical models. Consider a semi-infinite cylindrical gas body of uniform temperature and composition, emitting and absorbing radiative energy, as shown in Fig. 1. The gas body is separated from a differential area dA by a nonabsorbing medium. No scattering of radiation exists in the system. The spectral apparent emissivity, defined as the ratio of the radiative energy flux to that of a blackbody at the same temperature, is given as[1]

$$\epsilon_\lambda = \frac{1}{\pi}\int_\beta \int_\phi (1 - e^{-A_\lambda S}) \sin\beta \cos\beta d\beta d\phi \quad (1)$$

where $A_\lambda = a_\lambda r_0$, $S = (s/r_0)$, a_λ is the linear spectral absorption coefficient, r_0 the radius of the cylindrical body; and the path length s is a function of the height of shielding h, the radial distance in the base plane r, the azimuth angle ϕ, and the polar angle β. Thus, $S = S(H,R,\phi,\beta)$ and $\epsilon_\lambda = \epsilon_\lambda(H,R,A_\lambda)$, where $H = (h/r_0)$ and $R = (r/r_0)$.

Equation (1) can be rearranged into a different form as $\epsilon_\lambda = F - \epsilon_{\lambda c}$, where F is the configuration factor:

$$F \equiv \frac{1}{\pi}\int_\beta \int_\phi \sin\beta \cos\beta d\beta d\phi \quad (2)$$

and $\epsilon_{\lambda c}$ can be regarded as the contribution due to the finite absorption coefficient of the gas body

$$\epsilon_{\lambda c} \equiv \frac{1}{\pi}\int_\beta \int_\phi e^{-A_\lambda S} \sin\beta \cos\beta d\beta d\phi \quad (3)$$

A more convenient form for the integration of F and $\epsilon_{\lambda c}$ can be accomplished by introducing β', the projection of polar angle β onto the vertical plane, as shown in Fig. 1, where

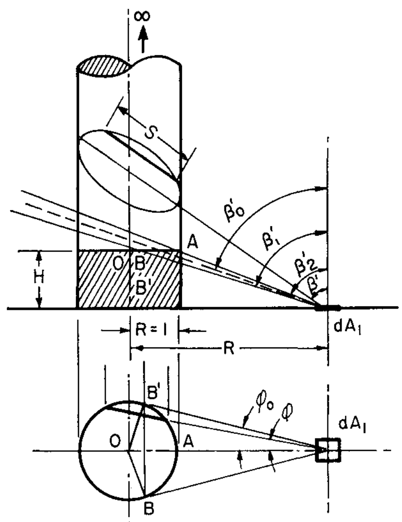

Fig. 1 Semi-infinite cylindrical gas body.

$\tan\beta = \sec\phi \tan\beta'$. Thus, the configuration factor can be written

$$F = \frac{2}{\pi}\int_0^{\beta_0'}\int_0^{\phi_0} \frac{\cos^2\phi \tan\beta' \sec^2\beta'}{(\cos^2\phi + \tan^2\beta')^2} d\beta' d\phi \quad (4)$$

where

$$\beta_0' = \frac{1}{2}\left[\tan^{-1}\left(\frac{R-1}{H}\right) + \tan^{-1}\left(\frac{R^2-1}{RH}\right)\right] \quad (5)$$

and $\phi_0 = \sin^{-1}(1/R)$. Equation (4) can be integrated directly by first integrating with respect to $\tan^2\beta'$ instead of β', and the result is

$$F(H,R) = \frac{1}{\pi}\sin\beta_0' \tan^{-1}(\sin\beta_0' \tan\phi_0) \quad (6)$$

The upper limit β_0', as illustrated in Fig. 1, is being approximated as the arithmetic mean of the two limiting angles β_1' and β_2' for the partially viewed region due to shielding. In the limiting case of $\beta_0' = \pi/2$ (corresponding to $H = 0$), an exact result is obtained for Eq. (6) with no shielding, $F(0,R) = (1/\pi)\sin^{-1}(1/R)$.

The term $\epsilon_{\lambda c}$ defined in Eq. (3) can be expressed from simple geometrical considerations as

$$\epsilon_{\lambda c}(H,R) = \frac{2}{\pi}\int_0^{\beta_0'}\int_0^{\phi_0} e^{-A_\lambda S}\frac{\cos^2\phi \tan\beta' \sec^2\beta'}{(\cos^2\phi + \tan^2\beta')^2} d\beta' d\phi \quad (7)$$

where the dimensionless path length, as shown in Fig. 1, is given by

$$S(R,\beta',\phi) = \frac{2}{\tan^2\beta'}(1 - R^2\sin^2\phi)^{1/2}(\cos^2\phi + \tan^2\beta')^{1/2} \quad (8)$$

The integral in Eq. (7) must be evaluated numerically at different locations specified by H and R. Two asymptotic expressions for $\epsilon_{\lambda c}$, however, can be obtained through direct integration. In the case of no shielding ($H = 0$), the asymptotic expression of ϵ_λ for $A_\lambda \ll 1$ is given as[2]

$$\epsilon_\lambda(0,R) = \frac{4A_\lambda}{\pi}\left[RE_2\left(\frac{\pi}{2},\frac{1}{R}\right) - \left(\frac{R^2-1}{H}\right)E_1\left(\frac{\pi}{2},\frac{1}{R}\right)\right] \quad (9)$$

where E_1 and E_2 are the elliptic integrals of the first and second kinds, respectively. For large R, the spectral apparent emissivity can be expressed as $\epsilon_\lambda(0,R) = A_\lambda/R$. For the case with shielding ($H \neq 0$), the result for $A_\lambda \ll 1$ and $R \gg 1$ can be derived as[2]

$$\epsilon_\lambda(H,R) = (A_\lambda/R)\sin\beta_0' \quad (10)$$

Presented as Preprint 64-60 at the AIAA Aerospace Sciences Meeting, New York, January 20–22, 1964; revision received March 25, 1964. The present work is supported by NASA George C. Marshall Space Flight Center, Huntsville, Ala., under Contract No. NAS 8-850.

* Assistant Professor, Department of Mechanical Engineering.
† Research Assistant, Department of Mechanical Engineering.